Novel Furochromone Derivatives: Synthesis and Anticancer Activity Studies

Senem Demir,[a] Cigdem Özen,[b] Meltem Ceylan-Ünlüsoy,[a] Mehmet Öztürk,[b] and Oya Bozdağ-Dündar[a]*

[a]Faculty of Pharmacy, Department of Pharmaceutical Chemistry, Ankara University, Ankara, Turkey
[b]Izmir Biomedicine and Genome Center, iBG-Izmir, Dokuz Eylul University, Izmir, Turkey
*E-mail: bozdag@pharmacy.ankara.edu.tr

Received November 6, 2018
DOI 10.1002/jhet.3508
Published online 00 Month 2019 in Wiley Online Library (wileyonlinelibrary.com).

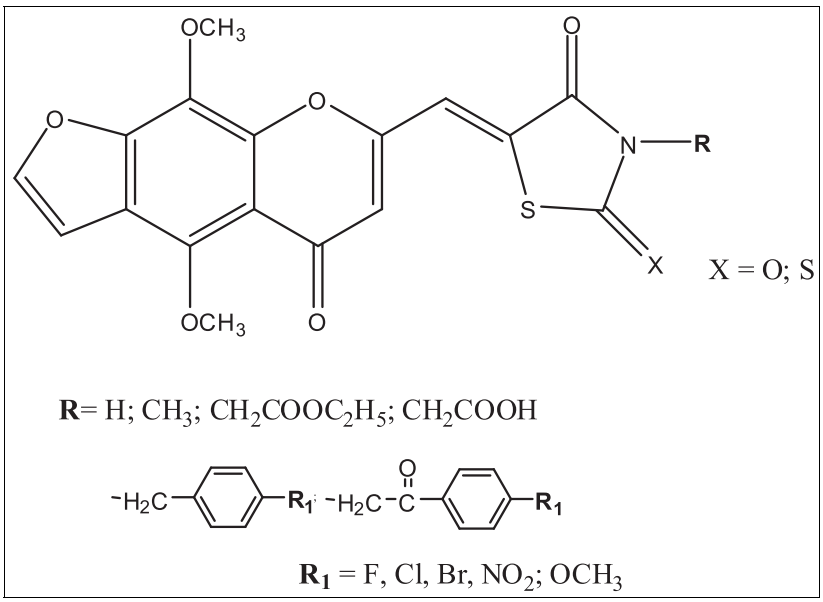

Medicinal plant extracts have been used for medical purposes throughout human history. In this study, khellin, having furochromone structure, which is obtained from a well-known traditional medicinal plant, was selected. A series of furochromonyl compounds (**K1**–**K14**) were synthesized for their anticancer activities. Furochromonyl compounds (**K1**–**K14**) were synthesized by Knoevenagel reaction of substituted 2,4-thiazolidinediones (**Ia**–**j**)/rhodanines (**Ik**–**n**) with khellin-2-carboxaldehyde (**V**), and their cytotoxicity was investigated in 22 cancer cell lines, which were originated from tissues such as the liver, breast, colon, and cervix. As the first step, two hepatocellular carcinoma cell lines Huh7 and PLC/PRF/5 (Alexander cells) were treated with 10 μM of each compound for 72 h, and then sulforhodamine B assay was performed to analyze their anti-growth activities. Ethyl 2-(5-((4,9-dimethoxy-5-oxo-5*H*-furo[3,2-*g*]chromen-7-yl)methylene)-4-oxo-2-thioxothiazolidin-3-yl)acetate (**K11**) was found as the most cytotoxic compound of primary screening. Afterwards, 12 hepatocellular carcinoma, seven breast cancer, two colon cancer, and a cervical cancer cell lines were selected to test **K11** for 72 h at multiple concentrations to determine 50% effective doses. Results showed that the 14 cell lines were affected by **K11** quantities lower than 10 μM. The structure of **K11**, which is particularly effective on breast cancers, can be used to slow down the progression of tumors. Furthermore, the discovery of more effective compounds can be carried out on the basis of this structure.

J. Heterocyclic Chem., **00,** 00 (2019).

INTRODUCTION

Cancer is a major public health problem, and it is known as the second leading death cause worldwide. Therefore, identification of novel potent, selective, and less toxic anticancer agents is essential for cancer therapy. Plants have a long history of use in the treatment of cancer, although many of the claims for the efficacy of such treatment should be viewed with some skepticism because cancer, as a specific disease entity, is likely to be poorly defined in terms of folklore and traditional medicine. Natural products are rich sources of anticancer agents and have significant impact on anticancer drug development. Plants are considered as important sources of anticancer drugs; therefore, there have been several natural compounds from higher plants currently being used as anticancer drugs or being evaluated in clinical trials [1,2].

The natural furochromone khellin (4,9-dimethoxy-7-methyl-5*H*-furo[3,2-*g*][1]benzopyran-5-one), a well-known traditional medicinal plant, which is also endemic to the Mediterranean region, is obtained from the fruits and seeds of *Ammi visnaga* (Apiaceae). Khellin possesses

high anti-atherosclerotic and lipid-altering activities, and it is the active constituent of many modern medicines [3,4]. Recently, anticancer activity of furochromone structure has been reported [5]. Thiazolidinedione (TZD) and rhodanine compounds have become very important groups of heterocyclic compounds in drug design and discovery. The present work has been endeavored aiming at designing and synthesizing novel 2,4-TZD or rhodanine compounds containing furochromone scaffold in their molecules to be pharmacologically screened for their anticancer activities (Figure 1).

Novel anticancer drug design is very popular. However, before the clinical trials, drug candidates should pass through *in vitro* cytotoxicity experiments in cancer cell lines. Because of the multi-disease nature of cancer, usage of more than one cancer cell is suggested. We basically used hepatocellular carcinoma (HCC), one of the most resistant tumor types against anticancer agents, as a model in this study [6,7]. Furthermore, breast, colon, and cervical cancer cell lines were also studied.

RESULTS

Chemistry. The synthetic protocol of khellin derivatives is shown in Schemes 1 and 2. 2,4-TZD (**Ia**) was synthesized with $ClCH_2COOH$ and thiourea in hot water [8]. Ethyl 2,4-dioxothiazolidin-3-yl acetate (**Ib**) was prepared *via* *N*-alkylation of 2,4-TZD (**Ia**) with ethyl bromoacetate in THF/NaH [9]. Substituted benzyl-2,4-TZDs (**Ic–f**) were obtained by 2,4-TZD (**Ia**) with appropriate benzylbromide derivatives in NaOH/ethanol. Substituted phenacyl-2,4-TZDs (**Ig–j**) were synthesized by reacting potassium 2,4-TZD (**Ia′**) with appropriate phenacylbromide derivatives in hot methanol. Ethyl 2-(4-oxo-2-thioxothiazolidin-3-yl)acetate (**Im**) was obtained from 2-(4-oxo-2-thioxothiazolidin-3-yl)acetic acid (**Ik**) by esterification reaction in ethanol/H_2SO_4 (Scheme 1).

Khellin-2-carboxaldehyde was synthesized from condensation of khellin (**II**) with 4-nitrosodimethylaniline (**III**) in the presence of sodium ethoxide, followed by hydrolysis of the obtained nitrone derivative (**IV**) with sulfuric acid, which afforded khellin-2-carboxaldehyde (**V**) [10].

Furochromone derivatives **K1–12** were prepared *via* Knoevenagel condensation reaction between khellin-2-carboxaldehyde (**V**) and suitable five-membered heterocyclic (**Ia–n**) in base condition (Scheme 2). Although piperidine was used as the base in this condensation for furochromonyl-3-benzyl or phenacyl substituted 2,4-TZDs (**K1–7**), CH_3COONa was more effective for the synthesis of other furochromone derivatives **K8–12**. The acidic hydrolysis of **K10** provided corresponding carboxylic acid **K13**. Compound **K14** was prepared *via* *N*-methylation of 2,4-TZD of compound **K8** with methyl iodide in NaH/DMF.

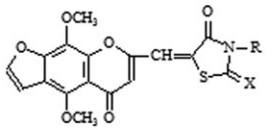

Comp.	X	R	Comp.	X	R
K1	O	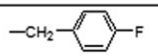	K2	O	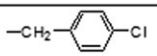
K3	O	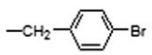	K4	O	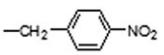
K5	O	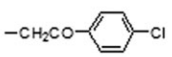	K6	O	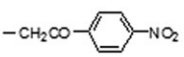
K7	O	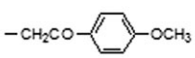	K8	O	H
K9	S	H	K10	O	$CH_2COOC_2H_5$
K11	S	$CH_2COOC_2H_5$	K12	S	CH_2COOH
K13	O	CH_2COOH	K14	O	CH_3

Figure 1. Synthesized khellin compounds **K1–K14**.

Scheme 1. Synthesis of starting compounds (**Ia–m**).

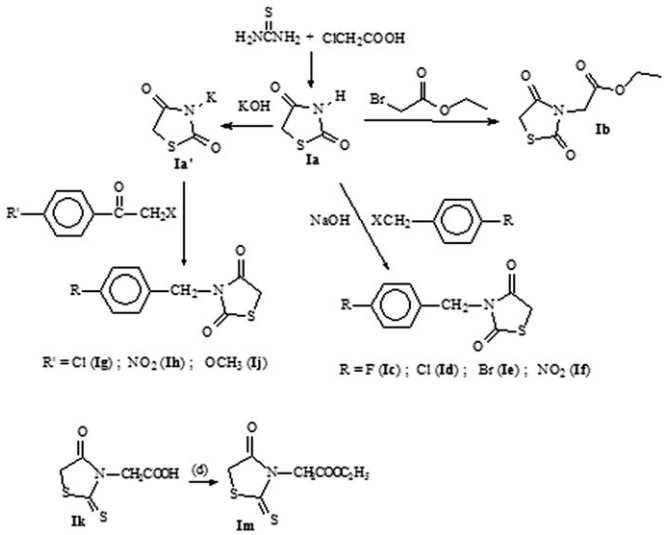

Scheme 2. Synthesis of khellin compounds **K1–K14**.

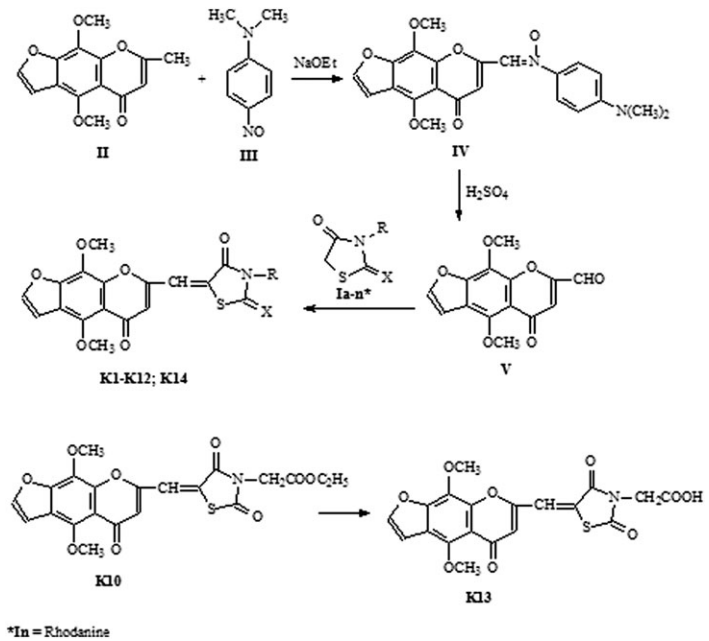

The structure of the synthesized furochromonyl compounds **K1–14** was elucidated by elementary analysis, ^{1}H-NMR, ^{13}C-NMR, and mass spectral data findings. All spectral data were in accordance with assumed structures. In ^{1}H-NMR spectra, furochromone protons were observed between 6.40 and 8.17 ppm, and methylene protons were seen at 7.35–7.87 ppm as a singlet. ^{13}C-NMR analysis of **K14** could not be performed because of **K14**'s poor solubility.

Biological activity. ***Initial screening and cell morphology.*** Novel khellin derivatives were initially screened for their cytotoxic effect on two HCC cell lines Huh7 and PLC/PRF/5 (Plc) by sulforhodamine B (SRB) assay; 10-μM compounds (**K1–K14**) were introduced as triplicates to two cell lines for 72 h. Initial screening results showed that **K11** was the most cytotoxic compound with more than 80% growth inhibition in Huh7 cells (Figure 2). Therefore, further investigation was carried out to understand effect mechanism of **K11**.

Morphological changes of cells that were treated with **K11** for 72 h were examined (Figure 3) for six cell lines [Huh7 (Figure 3a), Mcf7 (Figure 3b), HepG2 (Figure 3c),

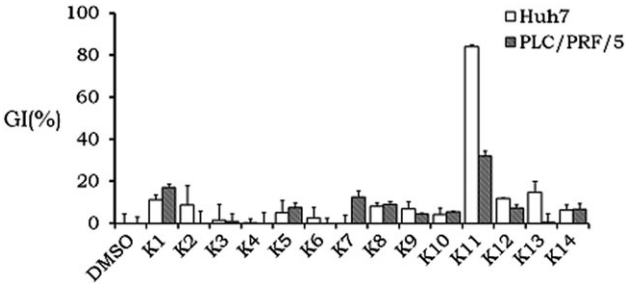

Figure 2. Initial screening of khellin derivatives; 10 μM of each khellin was applied in Huh7 and PLC/PRF/5 cells for 72 h. Sulforhodamine B assay was used following the steps that are detailed in the Experimental section. Cell density values were used to calculate growth inhibition (GI) percentages, and standard error of mean values were used for variable data indications of each compound. Dimethyl sulfoxide (DMSO) was used as negative vehicle control.

Snu449 (Figure 3d), Hep 3B (Figure 3e), and Plc/Prf/5 (Figure 3f)]. The obvious result was that almost all cells were stopped or destroyed in higher concentrations of **K11**. Huh7 and Mcf7 cell lines were found as the most sensitive cells (Figure 3a,b). Only HepG2 cells seemed resistant against high doses of **K11** (Figure 3c). HepG2 cell line has been described as well-differentiated HCC in the literature. Actually, this finding suggests that **K11** might be less toxic to normal liver cells than tumor cells.

Cell survival properties and IC_{50} determination. Twenty-two cell lines (12 HCC, seven breast cancer, two colons, and one cervical cancer) were used for calculation of 50% effective cytotoxic concentrations of **K11** (Table 1). Twelve HCC cell lines including Huh7, Plc, Hep3B, HepG2, Hep40, skHep1, Mahlavu, Focus, Snu449, Snu387, and Snu475; seven breast cancer cell lines including BT20, T47D, MDA MB 361, MDA MB 231, SK-BR3, Mcf7, and HCC1937; two colon cancer cell lines, SW620 and HCT116; and a cervical cancer cell line, HeLa, were cultured in the presence of a series concentrations of **K11** (2.5 to 40 μM) for 72 h. In the experiments, less than 1% DMSO was maintained with respective media for each cell line as a negative control; doxorubicin was also used as positive drug indicators in triplicate range of 1- to 4-μM concentrations, respectively.

Cell survival percentages were calculated by comparing optical density (OD) values for **K11** concentrations to vehicle control. In terms of cell survival decreases, Huh7 (Figure 4a), Hep 3B (Figure 3e), and Mcf7 (Figure 4a) cells were directly affected by **K11**, even less than 5 μM. Almost 90% Snu387 cells and 60% Hct116 were survived under 20-μM **K11** concentrations (Figure 4a).

Fifty percent effective dose or EC50 values were calculated by regression analysis between the probit values (corresponding to percent growth inhibition values) and **K11** concentrations (converted at the $\log_{10}$ base). EC50 values of **K11** showed that 14 cell lines were more affected by the presence of less than 10-μM **K11** (1.7–10 μM) (Table 1 and Figure 4b). The most **K11** tolerance belonged to Snu387 cell line, which is poorly differentiated type cancer cell line (Table 1 and Figure 4). In terms of sensitivity, the most sensitive cell lines were Mcf7 and Huh7; both have epithelial cell properties (Table 1 and Figures 3a,b and 4). Overall results showed that the growth rate of all tested breast cancer cell lines reduced by at least 50% at 10 μM or less of **K11** concentrations. In contrast, HCC cell lines were only affected by **K11** at higher concentrations (Figure 4b).

***Cell cycle changes after K11** treatment.* Propidium iodide (PI)-stained DNA content of the cells was read by flow cytometer to follow cell cycle progression after the drug candidate treatments. Cell fixation and staining protocol were followed as described in the experimental part.

When Huh7, Plc, and Snu449 cell lines were treated with 5- and 10-μM **K11** for 48 h (Figure 5a,b), Plc cell cycle was not changed in any phase. However, SubG1 and G2/M phases were increased in Huh7 in **K11** concentration-dependent manner. At low concentrations (5 μM) for the Snu449 cells, the S-G2/M phases increased significantly in the presence of **K11**, while SubG1 significantly increased in the high (10 μM) **K11** concentration.

Cell cycle response differences of HCT116 p53 wild-type ($p53^{+/+}$)(wt) and null ($p53^{-/-}$)(mt) isogenic colorectal cancer cell lines after **K11** treatment were determined by flow cytometer, and histograms were analyzed by FLOWING SOFTWARE 2.5.1 (Figure 6a,b). When we compared HCT116 isogenic cells, **K11** changed the cell cycle in both cells depending on concentration. After 48 h of administration, **K11** caused an increase in G2/M phase in p53 null cells and SubG1 phase in p53 wt cells.

DISCUSSION

Furochromones have been used as traditional medicine in Asia and the Middle East. Khellin is a furochromone, and it has anti-inflammatory and analgesic properties. Khellin derivatives have been used for the treatment of vitiligo and bronchial asthma [11]. In literature, studies on biological activities and cytotoxic action mechanism of khellin have been carried out by a number of research groups.

It was reported that furochromones modulate the expression and activity of cytochrome P450 1A1 (CYP1A1), which is a pro-carcinogen-activating enzyme in human HepG2 HCC cells and primary human hepatocytes. It was suggested that furochromones such as khellin and visnagin should be investigated for further toxicological characterization because of their possible

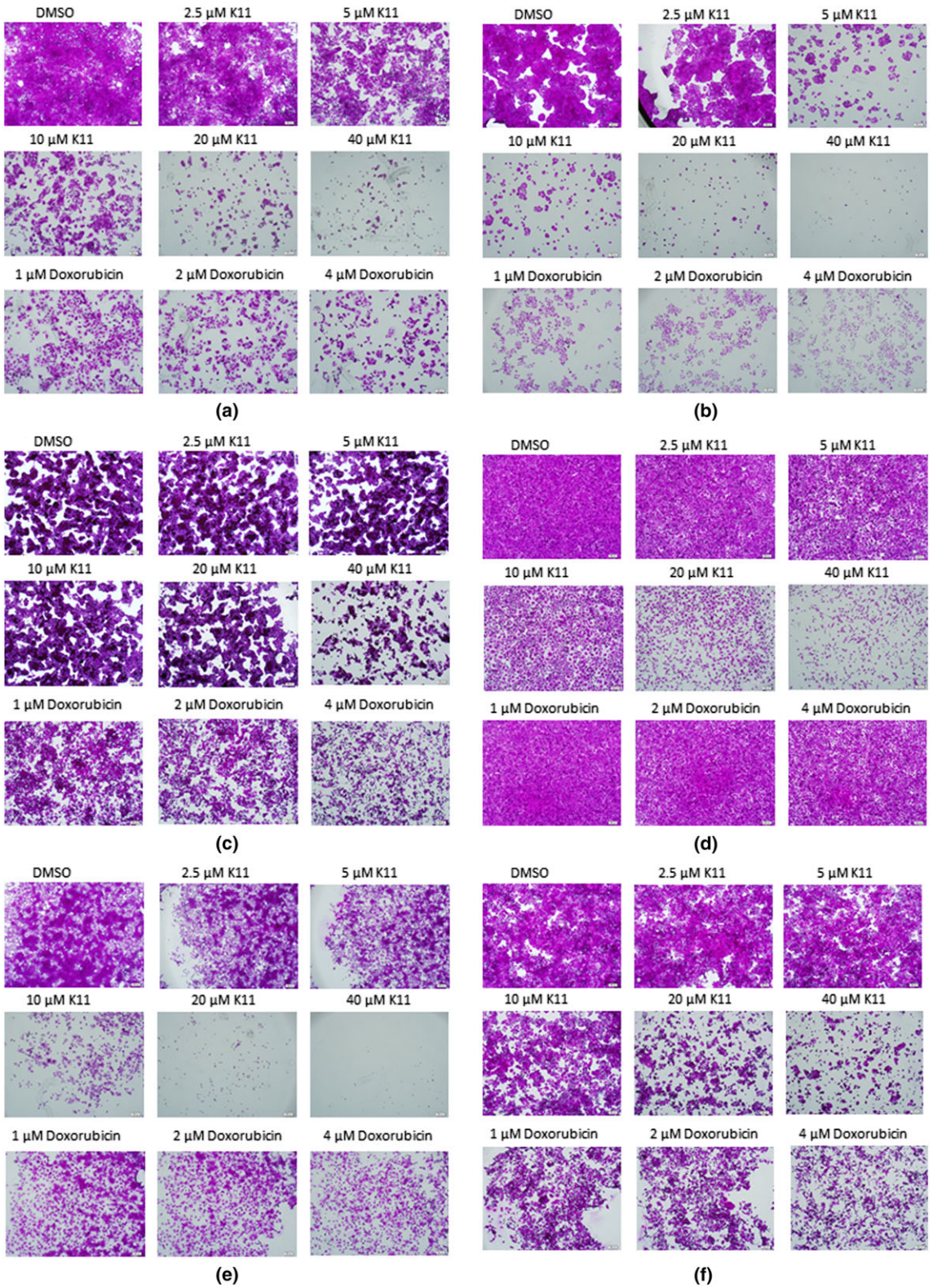

Figure 3. Concentration-dependent cell response in **K11**-treated cell lines [(a) Huh7, (b) Mcf7, (c) HepG2, (d) Snu449, (e) Hep3B, (f) Plc/Prf/5]; 2000–6000 cells were inoculated into 96-well plates. After overnight cultivation, the cells were incubated with dimethyl sulfoxide, **K11** (2.5, 5, 10, 20, and 40 μM), and doxorubicin (1, 2, and 4 μM) for 72 h. Cells were fixed by 10% trichloroacetic acid and stained with sulforhodamine B (SRB). Prior to the resuspension phase of the SRB assay, cell images were taken under an inverted phase-contrast microscope (4× magnification). [Color figure can be viewed at wileyonlinelibrary.com]

Table 1

Fifty percent effective concentration (EC50) values of the **K11** in 22 different cell lines.

Cancer cell type	Cell line	EC50 (μM)	±SD (μM)
Breast cancer	*Mcf7*	1.732	0.093
Breast cancer	*MDA MB 231*	2.912	0.765
Hepatocellular carcinoma	*Huh7*	3.797	0.085
Hepatocellular carcinoma	*Hep3B*	3.960	0.203
Breast cancer	*T47D*	4.067	0.057
Breast cancer	*SK BR3*	4.430	0.130
Breast cancer	*MDA MB 361*	4.744	0.155
Hepatocellular carcinoma	*Hep40*	4.932	0.027
Hepatocellular carcinoma	*skHep1*	6.328	0.098
Hepatocellular carcinoma	*Snu449*	6.883	0.027
Cervical carcinoma	*HeLa*	8.008	0.660
Colorectal carcinoma	*Sw620*	8.869	0.161
Hepatocellular carcinoma	*Snu398*	10.115	0.475
Breast cancer	*BT20*	10.171	0.213
Hepatocellular carcinoma	*Focus*	10.522	0.100
Breast cancer	*HCC1937*	10.557	0.222
Hepatocellular carcinoma	*Mahlavu*	12.897	0.131
Hepatocellular carcinoma	*Plc/Prf/5*	15.785	0.672
Hepatocellular carcinoma	*HepG2*	24.218	3.224
Hepatocellular carcinoma	*Snu475*	25.854	11.221
Colorectal carcinoma	*Hct116*	30.934	4.186
Hepatocellular carcinoma	*Snu387*	45.877	3.713

EC50 values were calculated by probit analysis of cell response curves. SD, standard deviation.

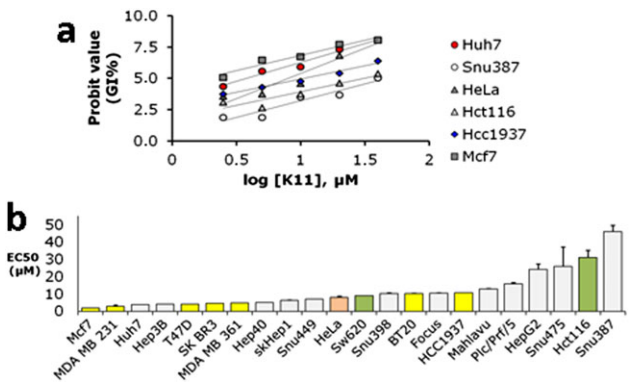

Figure 4. Probit-$\log_{10}$ (μM) plots (a) and EC50 comparison (b) in different cell lines. Growth inhibition values from sulforhodamine B readings were used for finding probit values from probit table. **K11** concentration values were transformed to $\log_{10}$ values. Probit versus $\log_{10}$ (μM) regression analysis was used for EC50 determination. The colors at plot (b) indicate as follows: gray, HCC; yellow, breast; pink, cervical carcinoma; and green, colon cancer cell lines. [Color figure can be viewed at wileyonlinelibrary.com]

toxic side effects [19]. Accordingly, we synthesized 14 different khellin derivatives and tested their cytotoxic potential against cancer cells.

It was also shown that some hetero aromatic benzofurans, which are derived from natural furochromone visnagin, had antitumor activities along with antimicrobial activities [12]. However, in another study, natural khellin was isolated from *A. visnaga*, and no cytotoxic effect of khellin could be found [13].

Recently, in a review article about furochromones, khellin's photoactivation potentials and adduct production of nucleic acids were pointed out [14].

The studies on khellin derivatives are increasing because of their potential cytotoxicity. However, there are few studies on exact action mechanism of khellin, and this problem has remained unsolved. Before going to the mechanism, khellin must be tested for their cytotoxicity potential. If they kill the cells or stop their growth, then the mechanism of action must be investigated in terms of anticancer properties. In this study, we wanted to see the cytotoxicity potentials in 22 cancer cell lines of 14 different khellin compounds, and these potentials were used as an advantage in favor of treating the cancer cells.

Indeed, **K11** [ethyl 2-(5-((4,9-dimethoxy-5-oxo-5H-furo[3,2-g]chromen-7-yl)methylene)-4-oxo-2-thioxothiazolidin-3-yl)acetate] was found to be highly cytotoxic against cancer cells that originated from different types of tissues.

Results showed that all of the tested cancer cells were active on the cell lines because of the concentration of **K11**. However, obtained cell cycle results suggest that, unlike doxorubicin, **K11** stops the growth of cells rather than putting them into the path of death. For this reason, it is believed that this compound structure may slow down the tumor growth in the treatment of cancer patients. It was highly effective on breast cancer cell lines than others; therefore, it is suggested that **K11** structure can be used for future design of novel breast cancer drugs.

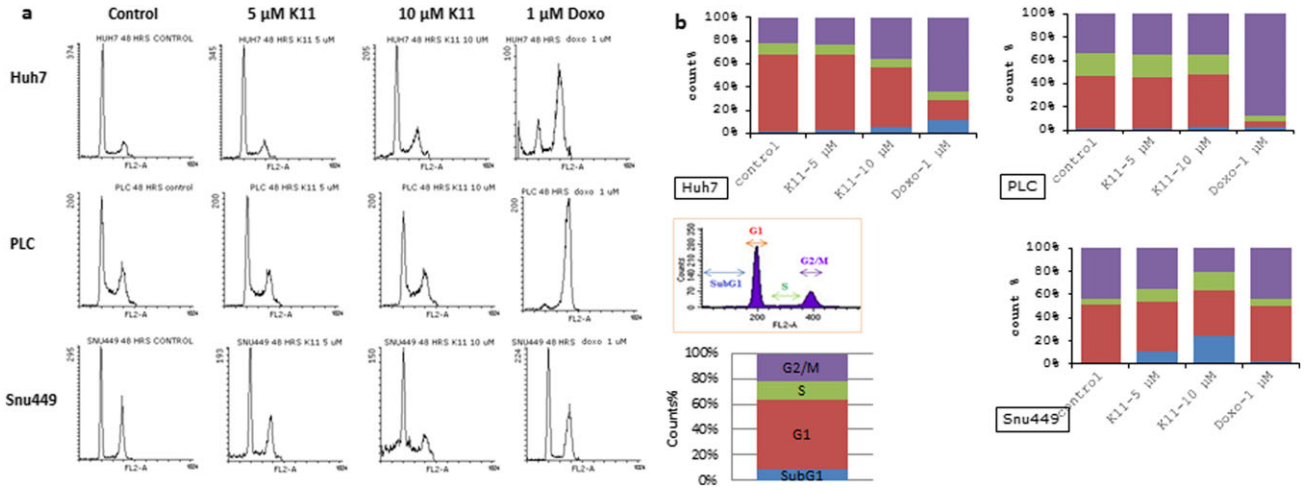

Figure 5. Cell cycle response differences in hepatocellular carcinoma. Propidium iodide staining of nucleic acids after **K11** treatment for 48 h in Huh7, Plc, and Snu449 cell lines. Shortly, cells were incubated with dimethyl sulfoxide (vehicle control), 5-μM **K11**, 10-μM **K11**, and 1-μM doxorubicin (positive control) containing media for 48 h. Seventy percent ice-cold ethanol-fixed cells were incubated with propidium iodide staining solution containing 0.5-mg propidium iodide, 0.2-mg RNase A, and 9.1% Triton X-100 for 40 min at 37°C in the dark. Cells were then washed with 1× phosphate-buffered saline (PBS) twice, and DNA content of the cells was measured through FL2 channel by flow cytometer. At least 10,000 cells were counted for each sample. Cell cycle histograms (a) were statistically analyzed with FLOWING SOFTWARE 2.5.1. Cell number percentages were compared (b). SubG1 phase implies apoptotic cells; G1 indicates G0–Gap1 phase cells in cell cycle; S indicates the cells during DNA replication; G2/M indicates the cells in Gap2 and cell division (mitosis). [Color figure can be viewed at wileyonlinelibrary.com]

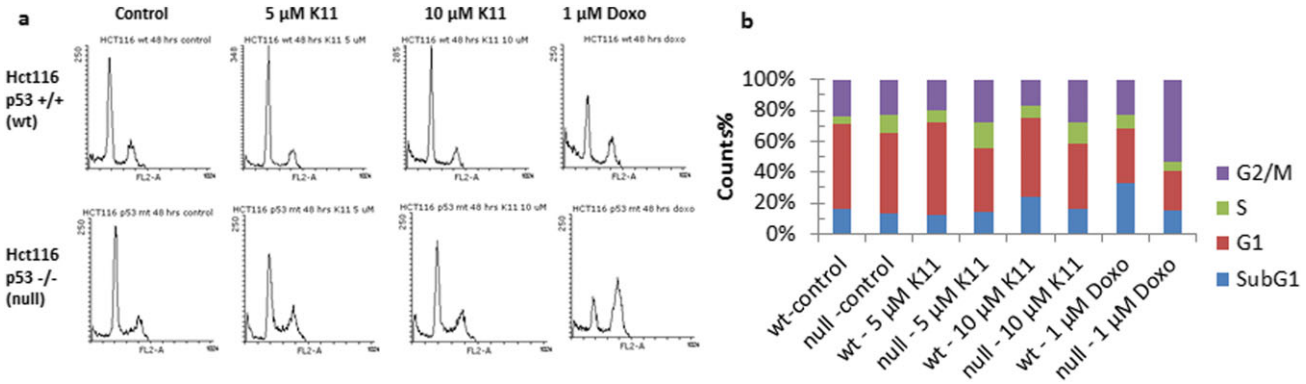

Figure 6. Cell cycle response differences of HCT116 p53 wild-type ($p53^{+/+}$)(wt) and null ($p53^{-/-}$)(mt) isogenic colorectal cancer cell lines after **K11** treatment. Shortly, cells were incubated with dimethyl sulfoxide (vehicle control), 5-μM **K11**, 10-μM **K11**, and 1-μM doxorubicin containing media for 48 h. Seventy percent ice-cold ethanol-fixed cells were incubated with propidium iodide staining solution containing 0.5-mg propidium iodide, 0.2-mg RNase A, and 9.1% Triton X-100 for 40 min at 37°C in the dark. Cells were then washed with 1× phosphate-buffered saline (PBS) twice, and DNA content of the cells was measured through FL2 channel by flow cytometer. At least 10,000 cells were counted for each sample. Cell cycle readings (a) were statistically analyzed with FLOWING SOFTWARE 2.5.1. Cell number percentages were compared (b). SubG1 phase implies apoptotic cells; G1 indicates G0–Gap1 phase cells in cell cycle; S indicates the cells during DNA replication; G2/M indicates the cells in Gap2 and cell division (mitosis). [Color figure can be viewed at wileyonlinelibrary.com]

All synthesized khellin compounds (**K1–14**) have furochromone ring as common part; they only have differences in heterocyclic moieties, which are TZD or rhodanine rings. It was found that the most potent compound was **K11**; therefore, activity mechanism studies of **K11** were carried out. The most potent compound **K11**'s structure was formed by connecting the methylene bridge of rhodanine ring to furochromone moiety; in addition, rhodanine ring is bearing the acetic acid ethyl ester group on rhodanine nitrogen instead of the hydrogen atom. Also, compounds **K9** and **K12** are rhodanine analogs of khellin, and they have no meaningful cytotoxic activity. In this case, in terms of cytotoxic activity, we can say that rhodanine ring is required, and this ring must bear a lipophilic group instead of acidic hydrogen.

As a conclusion, this study suggests that a form of furochromone, khellin, having a lipophilic rhodanine structure, must be considered seriously for designing new anticancer drug candidates.

EXPERIMENTAL

Chemistry. Melting points were measured on an Electrothermal 9100 type apparatus (Electrothermal Engineering, Essex, UK) and uncorrected. All instrumental analyses were performed in Central Laboratory of Pharmacy Faculty of Ankara University. ^{1}H-NMR and ^{13}C-NMR spectra were determined with a VARIAN Mercury 400 FT-NMR spectrometer (Varian Inc., Palo Alto, CA) in $CDCl_3$ and DMSO-d_6. All chemical shifts were reported as δ (ppm) values. Mass spectra were recorded on Waters Micromass ZQ (Waters Corporation, Milford, MA) by using ESI (+) method. Elementary analyses were performed on a Leco CHNS 932 analyzer (Leco, St. Joseph, MI), and satisfactory results of ±0.4% of calculated values (C, H, N) were obtained. For the chromatographic analysis, Merck Silica Gel 60 (230–400 mesh ASTM) was used. The chemical reagents used in synthesis were purchased from E. Merck (Darmstadt, Germany) and Aldrich (Milwaukee, MI). Khellin-2-carboxaldehyde (**V**) [10], 2,4-TZD (**Ia**) [8], substituted 2,4-TZD (**Ib–j**) [9,15–20], and **K1–K7** [21] were synthesized according to the literature.

Synthesis of ethyl 2,4-dioxothiazolidin-3-yl acetate (Ib). A mixture of 2,4-TZD (**I**) (2.5 g, 0.021 mol), ethyl bromoacetate (2.38 mL, 0.021 mol), and sodium hydride (0.512 g, 0.021 mol) in tetrahydrofuran 20 mL was stirred for 12 h at room temperature. The crude product was purified by column chromatography on silica gel eluting with dichloromethane : hexane (1:1); 2.8 g (64.55%) of **Ib** was obtained, mp: 44°C 9 (mp: 44°C).

General synthesis of compound Ic–f. A mixture of 2,4-TZD (**I**) (2.34 g, 0.02 mol), substituted benzyl halide (0.02 mol), and sodium hydroxide (0.8 g, 0.02 mol) in ethanol 20 mL was refluxed for 18 h. The crude product was crystallized from ethanol [**Ic** mp: 83°C 8 (mp: 82°C), **Id** mp: 95°C 15 (mp: 96°C), **Ie** mp: 91°C 16 (mp: 90–91°C), **If** mp: 117°C 17 (mp: 117°C)].

General synthesis of compound Ig–j. A solution of KOH (0.224 g, 0.004 mol) in CH_3OH (3 mL) was added dropwise to a suspension of 2,4-TZD (0.468 g, 0.004 mol) in 5 mL of CH_3OH. Ten minutes after this addition, 0.004 mol of substituted phenacyl bromide was added. The mixture was allowed to stand at room temperature over 5 min and then refluxed during 5 h. The crude product was removed by filtration and washed with H_2O and ether [**Ig** mp: 83°C 18 (mp: 82°C), **Ih** mp: 83°C 18 (mp: 82°C), **Ij** mp: 107.5°C 19 (mp: 107.5°C)].

Synthesis of ethyl 2-(4-oxo-2-thioxothiazolidin-3-yl)acetate (Im). A mixture of 2-(4-oxo-2-thioxothiazolidin-3-yl) acetic acid (**Ik**) [0.50 g (2.63 mmol)], ethanol (5 mL), and H_2SO_4 (0.5 mL) was refluxed for 7 h. The crude product was crystallized from ethanol. Yield: 0.445 g, 77.21%; mp: 60°C. Spectroscopic analysis: ^{1}H-NMR (δ ppm; $CDCl_3$): 1.29 (t, 3H, CH_3), 4.23 (q, 2H, CH_2), 4.08 (s, 2H, CH_2), 4.72 (s, 2H, CH_2). *Anal.* Calcd for $C_7H_9NO_3S_2$ C: 38.34, H: 4.14, N: 6.39, S: 29.25%; found: C: 38.53, H: 4.19, N: 6.47, S: 29.58%.

5,8-Dimethoxy-4′,5′-furo-6,7-chromone-2-carboxaldehyde (V). A solution of sodium ethoxide {Na°/abs. EtOH [44 mg (2 mmol)/15 mL]} was added dropwise to a cold (−5 to 0°C) solution of the khellin (**II**) (0.52 g, 2 mmol) and 4-nitroso-*N*,*N*-dimethylaniline (**III**) (0.9 g, 6 mmol) in absolute ethanol (10 mL), and the mixture was set aside at room temperature for 10 min. The red precipitate was collected and washed with ethanol and then with ether. The product was purified by column chromatography on silica gel eluting with chloroform; 0.28 g (34.31%) of **IV** was obtained, mp: 210°C 20 (mp: 210°C).

A mixture of nitrone derivative (**IV**) (0.25 g, mmol) and 5 M H_2SO_4 (2.5 mL) was stirred at room temperature for 15 min. After dilution with water (10 mL), the precipitate was collected and purified by column chromatography on silica gel eluting with chloroform; 0.10 g (71.43%) of **V** was obtained, mp: 180°C 10 (mp: 182–184°C).

General synthesis of compounds K1–K12. A mixture of **V** (0.001 mol) and **Ia–n** (0.001 mol) was refluxed in the presence of 5-mL ethanol and piperidine (0.001 mol) for 2 h. The precipitate was filtered and purified by column chromatography using CH_2Cl_2 as eluant.

3-(4-Fluoro-benzyl)-5-(5,8-dimethoxy-4′,5′-furo-6,7-chromone-2-ylmethylenyl)thiazolidine-2,4-dione (K1). Yield (%): 49.9, mp: 249°C. Spectroscopic analysis: ^{1}H-NMR (DMSO-d_6, 400 MHz, δ ppm): 3.95 (s, 3H, 8-OCH_3), 4.2 (s, 3H, 5-OCH_3), 4.8 (s, 2H, N–CH_2), 6.4 (s, 1H, 3-H), 6.9 (d, 2H, $j_{a,b} = j_{a',b'} = 8.5$ Hz, a,a′-H), 7.0 (d, 1H, $j_{3'2'} = 2.2$ Hz, 3′-H), 7.3 (d, 2H, $j_{b,a} = j_{b',a'} = 8.5$ Hz, b,b′-H), 7.5 (s, 1H, =CH), 7.6 (d, 1H, $j_{2'3'} = 2.3$ Hz, 2′-H) [21].

3-(4-Chloro-benzyl)-5-(5,8-dimethoxy-4′,5′-furo-6,7-chromone-2-ylmethylenyl)thiazolidine-2,4-dione (K2). Yield (%): 57.6, mp: 270°C. Spectroscopic analysis: ^{1}H-NMR (DMSO-d_6, 400 MHz, δ ppm): 4.0 (s, 3H, 8-OCH_3), 4.2 (s, 3H, 5-OCH_3), 4.8 (s, 2H, N–CH_2), 6.4 (s, 1H, 3H), 7.0 (d, 1H, $j_{3'2'} = 2.3$ Hz, 3′-H), 7.2 (d, 2H, $j_{a,b} = j_{a',b'} = 8.5$ Hz, a,a′-H), 7.3 (d, 2H, $j_{b,a} = j_{b',a'} = 8.5$ Hz, b,b′-H), 7.4 (s, 1H, =CH), 7.6 (d, 1H, $j_{2'3'} = 2.3$ Hz, 2′-H) [21].

3-(4-Bromo-benzyl)-5-(5,8-dimethoxy-4′,5′-furo-6,7-chromone-2-ylmethylenyl)thiazolidine-2,4-dione (K3). Yield (%): 45.2, mp: 264–266°C. Spectroscopic analysis: ^{1}H-NMR (DMSO-d_6, 400 MHz, δ ppm): 4.1 (s, 3H, 8-OCH_3), 4.3 (s, 3H, 5-OCH_3), 4.9 (s, 2H, N–CH_2), 6.5 (s, 1H, 3-H), 7.1 (d, 1H, $j_{3'2'} = 2.2$ Hz, 3′-H), 7.4 (d, 2H, $j_{a,b} = j_{a',b'} = 8.4$ Hz, a,a′-H), 7.5 (s, 1H, =CH), 7.51 (d, 2H, $j_{b,a} = j_{b',a'} = 8.4$ Hz, b,b′-H), 7.7 (d, 1H, $j_{2'3'} = 2.2$ Hz, 2′-H) [21].

3-(4-Nitro-benzyl)-5-(5,8-dimethoxy-4′,5′-furo-6,7-chromone-2-ylmethylenyl)thiazolidine-2,4-dione (K4). Yield

(%): 64.1, mp: 340–341°C. Spectroscopic analysis: ^{1}H-NMR (DMSO-d_6, 400 MHz, δ ppm): 4.1 (s, 3H, 8-OCH_3), 4.3 (s, 3H, 5-OCH_3), 5.0 (s, 2H, N–CH_2), 6.5 (s, 1H, 3-H), 7.1 (d, 1H, $j_{3'2'}$ = 2.3 Hz, 3′-H), 7.5 (s, 1H, =CH), 7.6 (d, 2H, $j_{a,b}$ = $j_{a',b'}$ = 8.7 Hz, a,a′-H), 7.7 (d, 1H, $j_{2'3'}$ = 2.3 Hz, 2′-H), 8.3 (d, 2H, $j_{b,a}$ = $j_{b',a'}$ = 8.7 Hz, b,b′-H) [21].

3-[2-(4-Chloro-phenyl)-2-oxo-ethyl]-5-(5,8-dimethoxy-4′,5′-furo-6,7-chromone-2-ylmethylenyl)-thiazolidine-2,4-dione (K5). Yield (%): 34.5, mp: 269–271°C. Spectroscopic analysis: ^{1}H-NMR (DMSO-d_6, 400 MHz, δ ppm): 4.0 (s, 3H, 8-OCH_3), 4.2 (s, 3H, 5-OCH_3), 5.1 (s, 2H, N–CH_2), 6.4 (s, 1H, 3-H), 7.0 (d, 1H, $j_{3'2'}$ = 2.3 Hz, 3′-H), 7.4 (d, 2H, $j_{a,b}$ = $j_{a',b'}$ = 8.5 Hz, a,a′-H), 7.5 (s, 1H, =CH), 7.6 (d, 1H, $j_{2'3'}$ = 2.3 Hz, 2′-H), 7.9 (d, 2H, $j_{b,a}$ = $j_{b',a'}$ = 8.5 Hz, b,b′-H) [21].

3-[2-(4-Nitro-phenyl)-2-oxo-ethyl]-5-(5,8-dimethoxy-4′,5′-furo-6,7-chromone-2-ylmethylenyl)thiazolidine-2,4-dione (K6). Yield (%): 71.7, mp: 344–345°C. Spectroscopic analysis: ^{1}H-NMR (DMSO-d_6, 400 MHz, δ ppm): 4.0 (s, 3H, 8-OCH_3), 4.2 (s, 3H, 5-OCH_3), 5.2 (s, 2H, N–CH_2), 6.4 (s, 1H, 3-H), 7.0 (d, 1H, $j_{3'2'}$ = 2.2 Hz, 3′-H), 7.5 (s, 1H, =CH), 7.6 (d, 1H, $j_{2'3'}$ = 2.3 Hz, 2′-H), 8.1 (d, 2H, $j_{a,b}$ = $j_{b',a'}$ = 8.8 Hz, a,a′-H), 8.3 (d, 2H, $j_{b,a}$ = $j_{b',a'}$ = 8.8 Hz, b,b′-H) [21].

3-[2-(4-Methoxy-phenyl)-2-oxo-ethyl]-5-(5,8-dimethoxy-4′,5′-furo-6,7-chromone-2-ylmethylenyl)-thiazolidine-2,4-dione (K7). Yield (%): 47.0, mp: 242–243°C. Spectroscopic analysis: ^{1}H-NMR (DMSO-d_6, 400 MHz, δ ppm): 3.9 (s, 3H, Ph-OCH_3), 4.1 (s, 3H, 8-OCH_3), 4.3 (s, 3H, 5-OCH_3), 5.2 (s, 2H, N–CH_2), 6.5 (s, 1H, 3-H), 7.0 (d, 2H, $j_{b,a}$ = $j_{b',a'}$ = 8.9 Hz, b,b′-H), 7.1 (d, 1H, $j_{3'2'}$ = 2.3 Hz, 3′-H), 7.6 (s, 1H, =CH), 7.7 (d, 1H, $j_{2'3'}$ = 2.3 Hz, 2′-H), 8.0 (d, 2H, $j_{a,b}$ = $j_{a',b'}$ = 8.9 Hz, a,a′-H) [21].

5-((4,9-Dimethoxy-5-oxo-5H-furo[3,2-g]chromen-7-yl) methylene)thiazolidine-2,4-dione (K8). Yield (%): 46.5, mp: 297°C. Spectroscopic analysis: ^{1}H-NMR (DMSO-d_6, 400 MHz, δ ppm): 3.96 (s, 3H, 8-OCH_3), 4.15 (s, 3H, 5-OCH_3), 6.75 (s, 1H, 3-H), 7.29 (d, 1H, 3′-H), 7.59 (s, 1H, =CH), 8.17 (d, 1H, 2′-H), 12.81 (s, 1H, NH); ^{13}C-NMR (DMSO-d_6, 100 MHz, δ ppm): 176.5 (CO), 169.1 (CO), 166.8 (CO), 156.5 (C), 148.9 (C), 147.3 (C), 146.9 (C), 145.8 (C), 131.9 (C), 129.4 (C), 122.1 (C), 119.2 (C), 115.7 (C), 113.4 (C) 105.3 (CH), 61.8 (O–CH_3), 61.4 (O–CH_3); MS (ESI+) *m/z* (rel. intensity): 374.0 (M + H, 100%); *Anal*. Calcd for $C_{17}H_{11}NO_7S$ C: 54.69, H: 2.97, N: 3.75, S: 8.59%; found: C: 54.58, H: 3.06, N: 3.85, S: 8.32%.

5-((4,9-Dimethoxy-5-oxo-5H-furo[3,2-g]chromen-7-yl) methylene)-2-thioxothiazolidin-4-one (K9). Yield (%): 52.8, mp: 323°C. Spectroscopic analysis: ^{1}H-NMR (DMSO-d_6, 400 MHz, δ ppm): 3.96 (s, 3H, OCH_3), 4.17 (s, 3H, OCH_3), 6.79 (s, 1H, 3-H), 7.30 (d, 1H, $j_{3'2'}$ = 2.4 Hz, 3′-H), 7.45 (s, 1H, =CH), 8.17 (d, 1H, $j_{2'3'}$ = 2.4 Hz, 2′-H); ^{13}C-NMR (DMSO-d_6, 100 MHz, δ ppm): 197.6 (CS), 176.4 (CO), 168.9 (CO), 156.2 (C), 148.8 (C), 147.3 (C), 146.9 (C), 145.7 (C), 133.7 (C), 129.3 (C), 121.1 (C), 119.1 (C), 116.2 (C), 113.3 (C), 105.3 (CH), 61.7 (O–CH_3), 61.3 (O–CH_3); MS (ESI+) *m/z* (rel. intensity): 389.40 (M + H, 100%); *Anal*. Calcd for $C_{17}H_{11}NO_6S_2$ C: 52.43, H: 2.85, N: 3.60, S: 16.47%; found: C: 52.04, H: 2.87, N: 3.73, S: 15.98%.

Ethyl 2-(5-((4,9-dimethoxy-5-oxo-5H-furo[3,2-g]chromen-7-yl)methylene)-2,4-dioxothiazolidin-3-yl)acetate (K10). Yield (%): 31.8, mp: 243°C. Spectroscopic analysis: ^{1}H-NMR ($CDCl_3$, 400 MHz, δ ppm): 1.31 (t, 3H, CH_3), 4.08 (s, 3H, OCH_3), 4.26 (q, 2H, CH_2O), 4.29 (s, 3H, OCH_3), 4.50 (s, 2H, N–CH_2), 6.45 (s, 1H, 3-H), 7.06 (d, 1H, $j_{3'2'}$ = 2.4 Hz, 3′-H), 7.52 (s, 1H, =CH), 7.69 (d, 1H, $j_{2'3'}$ = 2.4 Hz, 2′-H); ^{13}C-NMR ($CDCl_3$, 100 MHz, δ ppm): 177.7 (CO), 168.3 (CO), 166.1 (CO), 164.8 (CO), 156.4 (C), 149.4 (C), 147.6 (C), 146.2 (C), 146.1 (C), 130.5 (C), 129.9 (C), 124.4 (C), 120.4 (C), 116.6 (C), 114.2 (C), 105.5 (CH), 62.6 (O–CH_3), 62.5 (O–CH_3), 61.7 (O–CH_2), 42.4 (N–CH_2), 14.3 (CH_3); MS (ESI+) *m/z* (rel. intensity): 460.1 (M + H, 100%); *Anal*. Calcd for $C_{21}H_{17}NO_9S$ C: 54.90, H: 3.73, N: 3.05, S: 6.98%; found: C: 55.15, H: 3.88, N: 3.17, S: 6.95%.

Ethyl 2-(5-((4,9-dimethoxy-5-oxo-5H-furo[3,2-g]chromen-7-yl)methylene)-4-oxo-2-thioxothiazolidin-3-yl)acetate (K11). Yield (%): 60.6, mp: 235°C. Spectroscopic analysis: ^{1}H-NMR ($CDCl_3$, 400 MHz, δ ppm): 1.30 (t, 3H, CH_3), 4.08 (s, 3H, OCH_3), 4.25 (q, 2H, CH_2O), 4.33 (s, 3H, OCH_3), 4.87 (s, 2H, N–CH_2), 6.48 (s, 1H, 3-H), 7.06 (d, 1H, $j_{3'2'}$ = 2.0 Hz, 3′-H), 7.35 (s, 1H, =CH), 7.69 (d, 1H, $j_{2'3'}$ = 2.0 Hz, 2′-H); ^{13}C-NMR ($CDCl_3$, 100 MHz, δ ppm): 194.5 (CS), 177.8 (CO), 166.6 (CO), 165.8 (CO), 156.5 (C), 149.5 (C), 147.6 (C), 146.3 (C), 146.2 (C), 131.8 (C), 130.5 (C), 122.7 (C), 120.4 (C), 116.8 (C), 114.2 (C), 105.5 (CH), 62.7 (O–CH_3), 62.4 (O–CH_3), 61.7 (O–CH_2), 45.0 (N–CH_2), 14.3 (CH_3); MS (ESI+) *m/z* (rel. intensity): 476.1 (M + H, 100%); *Anal*. Calcd for $C_{21}H_{17}NO_8S_2$ C: 53.04, H: 3.61, N: 2.95, S: 13.46%; found: C: 52.62, H: 3.52, N: 3.17, S: 13.43%.

2-(5-((4,9-Dimethoxy-5-oxo-5H-furo[3,2-g]chromen-7-yl) methylene)-4-oxo-2-thioxothiazolidin-3-yl)acetic acid (K12). Yield (%): 50.3, decomp.p.: 320°C. Spectroscopic analysis: ^{1}H-NMR (DMSO-d_6, 400 MHz, δ ppm): 3.94 (s, 3H, OCH_3), 4.15 (s, 3H, OCH_3), 4.56 (s, 2H, N–CH_2), 6.81 (s, 1H, 3-H), 7.26 (d, 1H, $j_{3'2'}$ = 2.0 Hz, 3′-H), 7.65 (s, 1H, =CH), 8.14 (d, 1H, $j_{2'3'}$ = 2.4 Hz, 2′-H); ^{13}C-NMR (DMSO-d_6, 100 MHz, δ ppm): 194.9 (CS), 176.5 (CO), 166.9 (CO), 165.9 (CO), 156.1 (C), 148.8 (C), 147.3 (C), 146.9 (C), 145.7 (C), 130.0 (C), 129.3 (C), 123.0 (C), 119.1 (C), 116.6 (C), 113.3 (C), 105.3 (CH), 61.7 (O–CH_3), 61.4 (O–CH_3), 45.9 (N–CH_2); MS (ESI+) *m/z* (rel. intensity): 448.0 (M + H, 100%); *Anal*. Calcd for $C_{19}H_{13}NO_8S_2$-$2H_2O$ C: 47.20, H: 3.54, N: 2.90, S: 13.23%; found: C: 47.19, H: 3.34, N: 3.19, S: 12.84%.

2-(5-((4,9-Dimethoxy-5-oxo-5H-furo[3,2-g]chromen-7-yl) methylene)-2,4-dioxothiazolidin-3-yl)acetic acid (K13). A

mixture of acetic acid ester compound **2** (0.075 g, 0.163 mmol), glacial acetic acid (4 mL), and HCl (12 N, 1 mL) was refluxed for 2 h. After evaporation *in vacuo*, the residue was refluxed again with glacial acetic acid (4 mL) and HCl (12 N, 1 mL) for 2 h. After evaporation to dryness *in vacuo*, the crude solid was crystallized from ethanol, providing 0.055 g of pure carboxylic acid **K13**. Yield (%): 78.13, mp: 288°C. Spectroscopic analysis: ^{1}H-NMR (DMSO-d_6, 400 MHz, δ ppm): 3.45 (s, 2H, N–CH_2), 4.09 (s, 3H, OCH_3), 4.43 (s, 3H, OCH_3), 6.99 (s, 1H, 3-H), 7.17 (d, 1H, $j_{3'2'}$ = 2.0 Hz, 3′-H), 7.87 (s, 1H, =CH), 8.15 (d, 1H, $j_{2'3'}$ = 1.6 Hz, 2′-H), 13.01 (s, 1H, OH); ^{13}C-NMR (DMSO-d_6, 100 MHz, δ ppm): 183.3 (CO), 167.8 (CO), 167.6 (CO), 164.3 (CO), 159.1 (C), 150.8 (C), 148.9 (C), 147.0 (C), 144.1 (C), 129.9 (C), 125.7 (C), 123.7 (C), 113.8 (C), 113.6 (C), 105.7 (C), 104.4 (CH), 61.7 (O–CH_3), 42.6 (N–CH_2); MS (ESI+) *m/z* (rel. intensity): 432.0 (M + H, 50%); *Anal*. Calcd for $C_{19}H_{13}NO_9S$-1,5H_2O C: 49.78, H: 3.52, N: 3.06, S: 6.98%; found: C: 49.86, H: 3.18, N: 3.38, S: 7.06%.

5-[(4,9-Dimethoxy-5-oxo-5H-furo[3,2-g]chromen-7-yl) methylidene]-3-methyl-1,3-thiazolidine-2,4-dione (K14). A mixture of **K8** (0.090 g, 0.24 mmol), methyl iodide (0.068 g, 0.48 mmol), and sodium carbonate (0.026 g, 0.24 mmol) in DMF 5 mL was stirred for 5 h at room temperature. The crude product was purified by column chromatography on silica gel eluting with chloroform : ethyl acetate (5:3); 0.055 g (34.31%) **K14** was obtained. Yield (%): 70.68, mp: 314°C. Spectroscopic analysis: ^{1}H-NMR ($CDCl_3$, 400 MHz, δ ppm): 3.29 (s, 3H, CH_3), 4.08 (s, 3H, 8-OCH_3), 4.29 (s, 3H, 5-OCH_3), 6.44 (s, 1H, 3-H), 7.05 (d, 1H, 3′-H), 7.49 (s, 1H, =CH), 7.68 (d, 1H, 2′-H), 12.81 (s, 1H, NH); MS (ESI+) *m/z* (rel. intensity): 388.1 (M + H, 100%); *Anal*. Calcd for $C_{18}H_{13}NO_7S$ C: 55.81, H: 3.38, N: 3.62, S: 8.26%; found: C: 55.49, H: 3.51, N: 3.67, S: 7.87%.

Biological experiments. ***Preparation of stock solutions.*** All tested drug solutions were prepared as 5 mM in DMSO and stored in −20°C until use. Further dilutions of the compounds were prepared in respective media used for each cell line. Doxorubicine was used as a positive cancer drug indicator.

Cell lines and culture conditions. Two HCC cell lines, Huh7 and Plc/Prf/5 (Plc), were used for initial screening of all compounds. Twelve HCC cell lines (Huh7, Hep3B, Plc, HepG2, Mahlavu, Focus, SkHep1, Hep40, Snu449, Snu387, Snu475, and Snu398), seven breast cancer lines (Mcf7, HCC1937, BT20, MDA MB 361, SK-BR3, T47D, and MDA MB 231), two colon cancer cell lines (HCT116 and SW620), and one cervical cancer cell line (HeLa) were used for broader screening to calculate EC50 values. HCC cells were cultured at 37°C with 5% CO_2 in DMEM (Huh7, Hep3B, Plc, HepG2, Mahlavu, Focus, SkHep1, and Hep40) completed with 10% FBS, 1× NEA, 2-mM L-glutamine and 100 units penicillin/streptomycin except all Snu cell lines that were cultured in completed RPMI 1640. Breast cancer cell lines were cultured in the following completed media: DMEM was used for Mcf7, MDA MB 231, and BT20; DMEM plus sodium pyruvate was used for T47D and MDA MB 361; RPMI 1640 plus sodium pyruvate for HCC1937; and McCoy's for SK-BR3. Colon cancer cell lines were also cultured in the same conditions with McCoy's for Hct116 and DMEM for SW620. HeLa cell lines were cultured in completed DMEM.

Sulforhodamine B assay for cytotoxicity. Sulforhodamine B colorimetric protocol was carried out as described elsewhere with some modifications [22]. Before the experiments, initial cell numbers were optimized. Cell numbers, which could reach 0.800 to 1.2 OD in control wells, were used. These cell numbers (2000–10,000) are dependent on cell type and incubation time. Shortly, cells were cultured in 96-well plates for 24 h. After the incubation, fresh media with tested compounds were added onto the cells. When a 72-h incubation period was completed, media were discarded. Cells were washed with 1× phosphate-buffered saline (PBS) once and fixed by 10% trichloroacetic acid for 1 h at 4°C. Overnight dried plates were stained with 0.4% SRB in 1% acetic acid for 10 min at room temperature. To wash the excess of SRB, dye plates were washed with 1% acetic acid five times by tapping. Unbuffered 10-mM Trisma base solution was added to the wells to resolubilize the SRB dye. OD of each well was measured by μ-Quant microplate reader in a 405- to 515-nm wavelength range. Each concentration of the compounds was tested in triplicate. Average of OD values was used for calculation of growth inhibition percentages. Mean OD values were used for the calculation of growth inhibition percentages, and these percentages were normalized by probit transformation. The micromolar concentration values were converted on a $\log_{10}$ basis. Regression analysis was performed between the probit values of percent inhibitions and $\log_{10}$-based **K11** concentrations, and the **K11** concentration (or EC50 values) causing the 50% growth inhibition was calculated. The probit table was used to find the probit values.

Cell morphology changes. For each SRB experiment, before resolubilizing SRB with unbuffered tris, cell morphology of treated cell lines was photographed under the inverted phase contrast microscope.

Cell cycle analysis by flow cytometer. Preparation of fixed cells. For 24 h, 2.5×10^5 cells were cultured in six well plates. Cells were treated with desired concentrations of compound **K11** for 48 h. After the compound treatment, both the cells on the compound-containing media and

trypsinized cells were collected. After washing once with 1× PBS, cells were fixed by adding 70% ethanol during vortex. Fixed cells were kept in +4°C fridge at least 1 day.

Propidium iodide staining. Five hundred microliters of freshly prepared PI solution (50-μg/mL PI, 0.1-mg/mL RNase A, 0.05% Triton X-100 in 1× PBS) was applied for each sample for 45 min at 37°C in the dark. An excess amount of PI was washed with 1× PBS twice. Cells were resuspended with proper volume (500–1000 μL) of 1× PBS, and each sample was read by BD FACScalibur. For each condition, at least 10,000 cells were counted, and each sample was prepared as triplicates. Cell cycle differences were analyzed by FLOWING SOFTWARE 2.5.1 program.

CONFLICT OF INTEREST

The authors declare that there is no conflict of interest.

Acknowledgments. This work was supported by the Research Organization of Ankara University, Turkey (nos. 09B3336003 and 12B3336003). One of the authors was supported by Turkish Academia and Sciences (TUBA) DSAP program.

REFERENCES AND NOTES

[1] Cragg, G. M.; Grothaus, P. G.; Newman, D. J. Chem Rev 2009, 109, 3012.

[2] Cragg, G. M.; Newman, D. J. Biochim Biophys Acta 2013, 183, 3670.

[3] Sosnovskikh, V. Y.; Usachev, B. I. Tetrahedron Lett 2001, 42, 5121.

[4] Sellami, H. K.; Napolitano, A.; Masullo, M.; Smiti, S.; Piacente, S.; Pizza, C. Phytochemistry 2013, 95, 197.

[5] Galal, S. A.; Abd El-All, A. S.; Abdallah, M. M.; El-Diwani, H. I. Bioorg Med Chem Lett 2009, 19, 2420.

[6] Villanueva, A.; Hernandez-Gea, V.; Llovet, J. M. Nat Rev Gastroenterol Hepatol 2013, 10, 34.

[7] Germano, D.; Daniele, B. World J Gastroenterol 2014, 20, 3087.

[8] DeLima, M. C. A.; Costa, D. L. B.; Goes, A. J. S.; Galdino, S. L.; Pitta, I. R.; Luu-Duc, C. Pharmazie 1992, 47, 182.

[9] Rida, S. M.; Salama, H. M.; Labouta, I. M.; Ghany, Y. S. A. Pharmazie 1985, 40, 727.

[10] Mustafa, A.; Starkovsky, N. A.; Salama, R. I. J Org Chem 1961, 26, 886.

[11] Vrzal, R.; Frauenstein, K.; Proksch, P.; Abel, J.; Dvorak, Z.; Haarmann-Stemmann, T. PLoS One 2013, 8, e74917.

[12] El-Nakkady, S. S.; Roaiah, H. F.; El-Serwy, W. S.; Soliman, A. M.; El-Moez, S. I.; Abdel-Rahman, A. A. Acta Pol Pharm 2012, 69, 645.

[13] Cordero, C. P.; Gómez-González, S.; León-Acosta, C. J.; Morantes-Medina, S. J.; Aristizabal, F. A. Fitoterapia 2004, 75, 225.

[14] Abu-Hashem, A. A.; El-Shazly, M. Eur J Med Chem 2015, 90, 633.

[15] Goes, A. J. S.; DeLima, M. C. A.; Galdino, S. L.; Pitta, I. R.; Luu-Ducc, C. Ann Pharm Fr 1991, 49, 92.

[16] Costa, D. L. B.; Chantarel, J.; DeLima, M. C. A.; Albuquerque, J. F. C.; Lima, R. M. O.; Galdino, S. L.; Pitta, I. R.; Luu-Duc, C. J Pharm Belg 1995, 50, 5.

[17] Amorim, E. L. C.; Brandao, S. S. F.; Cavalcanti, C. O. M.; Galdino, S. L.; Pitta, I. R.; Luu-Duc, C. Ann Pharm Fr 1992, 50, 103.

[18] Salama, H. M.; Labouta, I. M.; Moustafa, M. A. Alex J Pharm Sci 1990, 4, 44.

[19] Ayhan-Kılcıgil, G.; Altanlar, N. Arzneim-Forsch/Drug Res 2000, 50, 154.

[20] Ayhan-Kılcıgil, G.; Tunçbilek, M.; Ertan, R.; Erol, K.; Yıldırım, E. Turk J Chem 2000, 24, 255.

[21] Bozdağ-Dündar, O.; Verspohl, E. J.; Waheed, A.; Ertan, R. Arzneim-Forsch/Drug Res 2003, 53, 831.

[22] Vichai, V.; Kirtikara, K. Nat Protoc 2006, 1, 1112.